Open Access

Advances in Chemical Research

Research Article

1-Decylbenzimidazole Copper(II) Complexes: Combined Experimental and DFT PCM and TD-DFT Computational Studies

Marek Łożyński †, Iwona Mądrzak-Litwa †, Aleksandra Borowiak-Resterna †,*

Institute of Chemical Technology and Engineering, Poznan University of Technology, ul. Berdychowo 4, 60-965 Poznań, Poland; E-Mails: marek.lozynski@put.poznan.pl; iwona-madrzak-litwa@wp.pl; aleksandra.borowiak-resterna@put.poznan.pl

† These authors contributed equally to this work.

* **Correspondence:** Aleksandra Borowiak-Resterna; E-Mail: aleksandra.borowiak-resterna@put.poznan.pl

Academic Editor: Maxim L. Kuznetsov

Special Issue: Coordination Chemistry and Metal Complexes

Advances in Chemical Research
2020, volume 2, issue 3
doi:10.21926/acr.2003007

Received: June 29, 2020
Accepted: August 13, 2020
Published: August 27, 2020

Abstract

1-Decylbenzimidazole (dbim) copper(II) complexes formed during solvent extraction were thoroughly studied, and their structures were predicted. Density functional theory (DFT) calculations of their structures and Time-dependent DFT (TD-DFT) calculations of their spectra indicated that 1-decylbenzimidazole forms both mono- and binuclear complexes with copper(II), with coordination numbers of 4 or 5. At the molar ratio of $[Cu(II)]_{aq}/[dbim]_{org} \geq 1$ and at $[Cl^-]_{aq} \geq 0.9$ mol dm^{-3} in the extraction media, a binuclear 1:1 square planar complex $[Cu_2Cl_4(dbim)_2]$ is expected as the main structure, in toluene solutions. However, at low chloride concentrations and a molar excess of the extractant in comparison to copper(II) in the extraction system, complexes with five-coordinated copper(II) centers are also feasible. With a large excess of extractant, chloride-free complexes may also form.

Keywords
1-Decylbenzimidazole; copper(II) complexes; solvent extraction; chloride solution; TD-DFT/PCM calculations

1. Introduction

Various transition metal complexes with 1-*H*-benzimidazole (simplified name: benzimidazole) and its derivatives are known. The metal ion binds *via* the nitrogen atom of the organic ligand in a monodentate [1-11] or multidentate [4, 12-16] coordination complex, the latter being formed when the benzimidazole derivative has more than two heteroatoms in the molecule (e.g., bibenzimidazoles or compounds having two benzimidazole units linked by carbon-heteroatom bridges). Usually, in these complexes, the benzimidazole ligands are bound to the metal ion by the imine nitrogen atoms. Besides, the coordination sphere of the central metal ion also contains anions, e.g., halides, NO_3^-, AcO^- etc. [1-7].

For monodentate benzimidazole ligands (*N*-unsubstituted or *N*-substituted benzimidazole), solid complexes having various structures have been isolated. The isolation is affected by both the experimental conditions and the nature of the central coordinating metal ion. It was found that zinc(II), cobalt(II), and copper(II) can form mononuclear complexes with *N*-unsubstituted benzimidazole in the presence of bromide or chloride ions. The metal ion is coordinated tetrahedrally to two halide anions and two benzimidazole ligands [1-5]. Intermolecular hydrogen bonds N-H···X and C-H···X were observed in the crystal complexes [1-3]. Four-coordinated zinc(II) and cobalt(II) complexes were obtained by Sireci et al. for the *N*-phenyl derivative of benzimidazole [6]. However, Tosik et al. synthesized unsymmetrical dihalo-bridged dinuclear five-coordinated copper(II) complexes $[Cu_2X_3L_5]X{\cdot}4H_2O$ (X = Cl or Br, L = benzimidazole), in which the complex cation $[Cu_2X_3L_5]^+$ was formed by two trigonal-bipyramidal copper(II) centers [7, 8]. Doo Hwan Jeong *et al*. obtained dinuclear copper(II) complexes in the reaction between copper(II) chloride and 1-alkylbenzimidazole (R = methyl or benzyl) where each five-coordinated copper(II) ion was bonded to one terminal, two bridging chlorides, and two 1-alkylbenzimidazole nitrogen atoms [9].

Some hydrophobic derivatives of benzimidazole are proposed as extractants of heavy metal ions. Devonald et al. [11] extracted copper(II) and zinc(II) from aqueous solutions using benzimidazole derivatives containing three types of substituents (alkanoyl, alkyloxycarbonyl, and 4-alkylbenzene sulfonyl) at position 1. The effect of methyl, chloride, and nitro groups in the 2, 5, or 6 positions of the extractant molecules during the extraction of HCl and metal ions from concentrated chloride solutions (3.6-10.8 mol dm^{-3} Cl^-) was investigated. The extraction properties of compounds with two benzimidazole units linked by carbon-heteroatom bridges were investigated by Kinnear *et al*. [13], Lockhart, and Rushton [14], and Matthews et al. [15] using three-phase transport techniques. The hydrophobicity of the compounds under consideration was increased by introducing a diakylamide [13, 15] or alkyl [14] group at the 1-position in the imidazole rings. These multidentate ligands formed complexes with bromide, perchlorate or nitrate salts of heavy metals (Cu(II), Ag(I), Zn(II), Cd(II), Pb(II)) in which the molar ratio of metal ions to the organic ligand equals to 1 [12-14]. However, to the best of our knowledge, there are no reports on the solvent extraction of copper(II) from aqueous solutions by 1-alkylbenzimidazoles as extractants. To date, the influence of the

extraction conditions on the structure of benzimidazole derivative complexes formed in a two-phase system has not been studied. However, this knowledge is essential in the design of cost-effective hydrometallurgical processes for the recovery of metals from aqueous solutions. There is scarcity in structural information on complexes formed in two-phase systems, but knowledge on structural properties is extremely interesting and useful in practice.

We report the study on the equilibrium of copper(II) extraction from a chloride solution by a hydrophobic alkyl benzimidazole derivative. 1-Decylbenzimidazole (dbim, Figure 1), used in our experiments, has two nonequivalent heterocyclic nitrogen atoms: an alkylated nitrogen to ensure good solubility of the extractant in an organic solvent, and active imine nitrogen. The structure of the benzimidazole derivative, where one nitrogen atom is substituted by a long alkyl chain, allows for efficient metal-ion complexation with only the nonalkylated imine nitrogen. Thus, the *N*-alkyl derivative of benzimidazole operates as a monodentate ligand and can compete in the interphase with chloride ions. To investigate the equilibrium of complexes formed in the toluene/aqueous two-phase system, both extraction and computational methods were done. In the computational experiments, the long alkyl group was replaced with a methyl substituent.

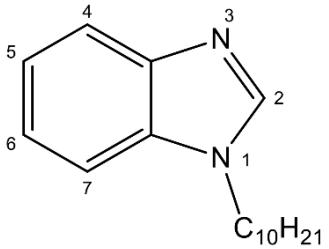

Figure 1 Structure of 1-decylbenzimidazole (dbim).

2. Materials and Methods

2.1 Materials

2.1.1 Reagents

Analytical grade copper(II) chloride (dehydrate), lithium chloride (monohydrate) (Chempur, Poland), lithium nitrate (anhydrous) (Acros Organics, Belgium), copper(II) nitrate (trihydrate), sodium chloride, sodium nitrate, hydrochloric acid (36%), and nitric acid (65%) (POCH, Poland) were used to prepare aqueous solutions. Deionized water and analytical grade toluene (POCH, Poland) were used as diluents.

2.1.2 Extractant

1-Decylbenzimidazole (dbim) was obtained by reacting benzimidazole with decyl bromide in the presence of sodium hydroxide in DMF [17]. The structure and purity were confirmed by high-resolution mass spectrum (HRMS), ^{1}H NMR, and ^{13}C NMR spectra. HRMS were acquired on an Intectra Mass AMD 402 spectrometer with electron-impact ionization, and 70 eV energy and NMR were done with a Bruker DRX 500 MHz spectrometer (500 and 125 MHz) in $CDCl_3$ using tetramethylsilane (TMS) as an internal reference.

The spectral characteristics of dbim are as follows:

yield 86%; thick light orange liquid; ^{1}H NMR ($CDCl_3$): δ 0.85 (t, *J*=7.0 Hz, 3H, CH_3), 1.22 (m, 14H, 7×CH_2), 1.85 (m, 2H, CH_2), 4.12 (t, *J*=7.5 Hz, 2H, NCH_2), 7.85 (s, 1 H, C2-H), 7.78 (dd, *J*=7.0 Hz, 1H, C4-H), 7.36 (dd, *J*=7.5 Hz, 1H, C7-H), 7.26 (m, 2H, C5-H and C6-H); ^{13}C NMR ($CDCl_3$): δ 13.59, 22.14, 26.27, 28.56, 28.72, 28.89, 28.94, 29.26, 31.32, 44.54, 109.17, 119.77, 121.45, 122.23, 133.30, 142.39, 143.32; HRMS. Calcd for $C_{17}H_{26}N_2$ (M^+): *m/z* 258.2096. Found: *m/z* 258.2087.

2.2 Methods

2.2.1 Acid Transfer to the Organic Phase

The compound ([dbim] = 0.2 mol dm^{-3}) in toluene was shaken with aqueous solutions containing [HCl] = 0.001-4.0 mol dm^{-3} and [LiCl] = 4.0 mol dm^{-3}.

The organic and aqueous solutions (1:1 by volume) were shaken for 2 h at 20-23 °C. The phases were separated. The acid concentration was determined in the organic phases (after filtration) by titration with a 0.01 mol dm^{-3} sodium hydroxide solution in ethanol. Bromothymol blue was used as an indicator.

2.2.2 Solvent Extraction Procedure

Extraction from weakly acidic chloride solutions (pH > 2.2) was carried out at a constant water activity (a_w = 0.835), a constant total concentration of ions and molecules dissolved in the aqueous solution ((σ = 8.0 mol dm^{-3}), [NaCl] + [$LiNO_3$] + [$NaNO_3$] = 4.0 mol dm^{-3}). The composition of the studied aqueous solutions was the same as reported by Cote et al. [18]. The chloride concentration was varied in the range of 0-4.0 mol dm^{-3}. The copper(II) chloride concentration in the aqueous phase was 0.40, 0.10, or 0.01 mol dm^{-3}. The concentration of dbim in toluene was 0.1 mol dm^{-3}.

The extraction of metal ions was carried out at 20-23 °C. The aqueous and organic (toluene) phases (1:1 by volume) were shaken in a glass test tube for 15 min (using Bio-mix BWR 04 instrument). The time required for attaining the extraction equilibrium did not exceed 5 min. Subsequently, the phases were separated. The copper(II) concentration was determined in the aqueous phases by atomic absorption spectrometry (AAS) using a Z8200 polarized Zeeman apparatus (Hitachi).

pH Values were measured using a 713 pH meter (Metrohm).

2.3 Calculations

The metal ion concentrations in the aqueous solutions before and after solvent extraction were analyzed by AAS. The concentrations of metal ions in the organic phase were determined by mass balance. The distribution ratio of metal ions (*D*), and extraction percentage (%*E*) were calculated from the following equations (assuming constant phase volumes):

$$D = \frac{\mathrm{c_{org}}}{\mathrm{c_{aq}}} \quad (1)$$

where c_{org} and c_{aq} are the total metal ion concentrations in the organic and aqueous phases, respectively, after extraction (in equilibrium).

$$\%E = \frac{D}{D + \frac{V_{aq}}{V_{org}}} \times 100 \quad (2)$$

If the phase volumes do not change and $V_{aq} = V_{org}$, Eq. (2) assumes a simpler form:

$$\%E = \frac{D}{D + 1} \times 100 \quad (3)$$

2.4 Computational Details

The tentative structures were optimized at the DFT level with the B3LYP hybrid functional as this gives reasonably accurate geometries [19, 20]. To obtain better estimates of the molecular geometries and energies, calculations were performed with diffusion functions at the B3LYP/6-31++G(d,p) level, which is a compromise between the size of the studied system and the computational demand. The loose convergence criteria were used (requiring the root-mean-square forces to be smaller than $1.667 \cdot 10^{-3}$ Hartree $Bohr^{-1}$). The absence of imaginary frequencies during frequency calculations at the B3LYP/6-31G(d) level confirmed that all the optimized structures were true minima. The quantum chemical modeling of the predicted complexes was performed without coordinated water molecules because an approximate number of coordinated water molecules could not be estimated. To estimate the geometry and relative energy changes in the solution, and to avoid the problem of solvent effects on solutes, we used the default integral equation formalism polarizable continuum model (IEF-PCM) [21]. The time-dependent DFT (TD-DFT) [22-26] was used to interpret the low lying bands of spectra of toluene benzimidazole extracts of copper(II) from an aqueous solution. All geometries in the gas phase and toluene and water environments were studied without symmetry constraints.

All calculations were performed with the Gaussian09 quantum chemistry package. DFT-optimized geometries of Cu(II) complexes were visualized by the GaussView package.

3. Results

3.1 Transfer of HCl to the Organic Phase

Depending on the acidity of aqueous solutions containing transition metal ions, heterocyclic extractants (e.g., pyridine, benzimidazole, or 2,2'-bibenzimidazole derivatives) may exhibit different extraction properties for different metal ions [27-29]. So, the ability of 1-decylbenzimidazole (dbim) to transfer hydrogen ions from aqueous solutions with different acidities was initially investigated.

The concentration of hydrochloric acid in the aqueous phase has a significant effect on the acid transfer to the toluene phase by dbim molecules (Table 1). Dbim, as a heterocyclic base, has a strong affinity for hydrogen ions. When the HCl concentration in the aqueous solution increases from 0.001 to 0.05 mol dm^{-3}, the acid concentration in the organic phase also rises. However, at higher HCl concentrations (above 0.05 mol dm^{-3}), a third oil phase is observed in the extraction system. The organic phase splits into two layers, a light toluene-rich phase, and a heavy extractant-rich phase. It is presumed that the separation of the third phase is caused by changes in the microscopic structure of the organic solution due to the aggregation of protonated extractant molecules [30].

Table 1 Acid transfer to the toluene phase by 1-decylbenzimidazole ($[dbim]_{org}$ = 0.2 mol dm^{-3}, $[LiCl]_{aq}$ = 4.0 mol dm^{-3}).

Starting HCl concentration in aqueous phase, mol dm^{-3}	0.001	0.010	0.050	0.1	0.5	1.0	2.0	3.0	4.0
Equilibrium HCl concentration in organic phase, 10^3 mol dm^{-3}	1.0	9.8	38.8	29.8*	9.4*	6.9*	5.6*	5.6*	5.0*

* The concentration in the light toluene-rich phase.

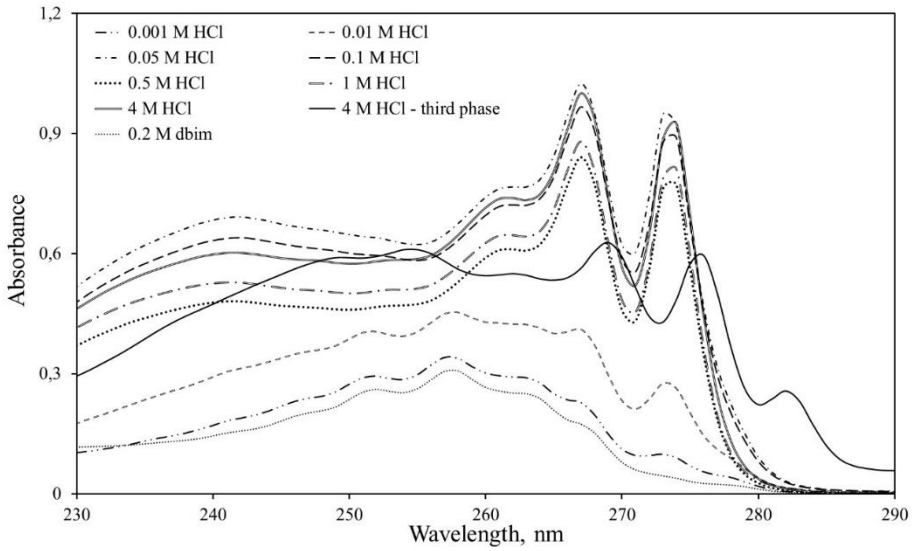

Figure 2 UV spectra of aqueous solutions after HCl extraction by 1-decylbenzimidazole (dbim) in toluene.

UV spectra of the aqueous solutions after hydrochloric acid extraction show that absorbance in the range of 250-274 nm rises with an increase in the aqueous HCl concentration from 0.001 to 0.05 mol dm^{-3}(Figure 2). However, the UV spectra of 0.001-0.01 mol dm^{-3} HCl in the aqueous phase after extraction are very similar to the spectrum of free 1-decylbenzimidazole (dbim) in the aqueous solution, obtained after extraction in 0.2 mol dm^{-3} $dbim_{toluene}$/4.0 mol dm^{-3} $LiCl_{aq}$. The UV spectrum of dbim in the aqueous solution after extraction shows a few bands at 252, 258 (highest in intensity), 262-263, 266-267, and 273 nm (shoulders). This confirms that at $[HCl]_{feed} \leq 0.01$ mol dm^{-3}, almost all of the acid is transferred into the organic phase (Table 1), and the aqueous phases after extraction contain mainly the free extractant and toluene. A few bands observed in the range 240-280 nm are characteristic for the intra-extractant $\pi \rightarrow \pi^*$ and $n \rightarrow \pi^*$ electron transitions (mainly of the free extractant molecules) and intramolecular toluene $\pi \rightarrow \pi^*$ electron transitions. However, for $[HCl]_{feed}$ = 0.05-4.0 mol dm^{-3}, after extraction, in the UV spectra of aqueous phases, a hyperchromic effect is observed with three intense bands at 262, 267, and 274 nm. This is due to the presence of a protonated extractant in the aqueous phases. Importantly, our absorption data on dbim after extraction is similar to the absorption spectrum of benzimidazole in 0.01 mol dm^{-3} HCl reported by Steck et al. [31] in acidic aqueous phases. However, it should be noted, that as much as 78% of the acid is transferred into the organic phase for $[HCl]_{feed}$ = 0.05 mol dm^{-3}, and a further increase in the concentration of HCl in the aqueous solution before the extraction causes the separation of the organic phase into two layers. The lower layer contains the protonated dbim. The UV spectrum of

the dense extractant-rich phase in ethanol shows very broad bands with their maxima at 249, 255, 262, 269, 276, and 282 nm (Figure 2). We presume that, at $[HCl]_{feed}$ > 0.05 mol dm^{-3}, a monohydrochloride of dbim (LH^+Cl^-, L = free dbim molecule) or its dihydrochloride, ($LH^+HCl_2^-$), possibly in the form of an ion pair coexists [32, 33]. Also, the physicochemical and compositional changes of the two organic layers with increasing initial aqueous HCl concentration are presumably the cause of the varying concentration of the protonated extractant in the aqueous phase.

3.2 Extraction of Copper(II) from Chloride Solution with 1-Decylbenzimidazole (dbim)

The extraction of copper(II) from chloride media at pH > 2.2 was carried out at a constant water activity (a_w = 0.835) and a constant total concentration of ions and molecules dissolved in the aqueous solution (σ = 8.0 mol dm^{-3}). Constant a_w and σ levels eliminate the effect of the aqueous phase composition on the activity coefficients of ions and molecules in the extraction media [18]. Lithium and sodium nitrates were used to adjust the activity of the water because nitrate ions form weaker complexes with Cu(II) than chloride ions. For example, the formation equilibrium constant of $CuNO_3^+$ at 25 °C is 0.07 ±0.02, which is in the range of nitrate concentrations considered in this study [34].

The influence of the chloride ion concentration on the extraction of copper(II) by dbim shows that the extraction of Cu(II) slightly increases when the NaCl concentration in the aqueous phase increases (Figure 3). A greater effect of the chloride ion concentration is observed at the molar ratio of $[Cu(II)]_{aq}/[dbim]_{org}$ = 1.0. The extraction percentage increases from 42% at 0.1 mol dm^{-3} NaCl to 60% at 4.0 mol dm^{-3} NaCl. Although Cu(II) ions form weaker complexes with nitrate than chloride ions, dbim also forms complexes with copper(II) in the systems devoid of chloride ions, but the nitrate concentration is equal to 4.0 mol dm^{-3} (copper(II), lithium, and sodium nitrates were used to prepare the feed).

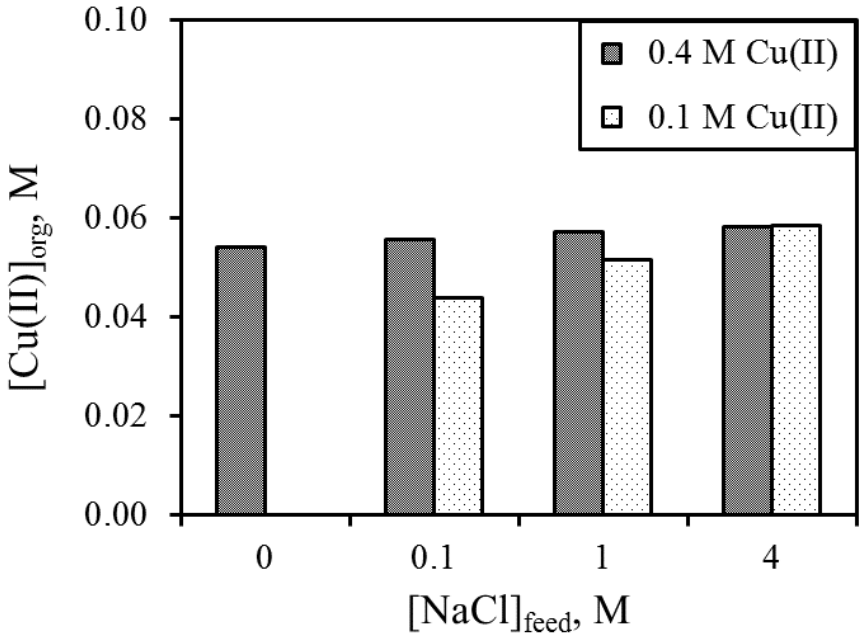

Figure 3 Influence of sodium chloride and copper ion concentrations on Cu(II) extraction from aqueous chloride/nitrate solutions by dbim ([dbim] = 0.1 mol dm^{-3}; pH of feed 2.2-3.3).

When $[Cu(II)]_{aq}/[dbim]_{org}$ = 1.0 mol mol^{-1}, the capacity of dbim increases from 0.44 to 0.60 mol Cu(II)/mol extractant when the NaCl concentration in the feed increases from 0.1 to 4.0 mol dm^{-3} (Figure 3). However, at $[Cu(II)]_{aq}/[dbim]_{org}$ = 4.0 mol mol^{-1}, at the same range of NaCl concentration, the capacity is always greater than 0.5 (0.55-0.60 mol Cu(II)/mol extractant).

3.3 Experimental UV-VIS Spectra

The electronic spectra of the toluene phases after Cu(II) extraction from the weakly acidic chloride solution with dbim were recorded between 200-1000 nm. Characteristic intra-ligand transitions and metal-to-ligand charge-transfer transition bands in the range of 280-450 nm, with a few high-intensity bands centered around 295-310, 345-360, and 390-405 nm were observed in all studied absorption spectra.

As shown in Table 2, the position of the bands in the visible range (600-1000 nm) depends on the [Cu(II)]/[extractant] concentration ratio in the extraction system as well as on the concentration of chloride ion s. The broad band in the 863-873 nm region with a pronounced shoulder between 794-798 nm is observed in the spectra of the toluene phase after Cu(II) extraction ($[Cu(II)]_{aq}/[dbim]_{org}$ = 1.0-4.0 mol mol^{-1} and $[Cl^-]_{aq} \geqslant$ 0.9 mol dm^{-3}) (Table 2, entries 1-4). When the concentration of chloride ions in the extraction system is reduced to 0.3 mol dm^{-3} and the molar ratio $[Cu(II)]_{aq}/[dbim]_{org}$ is 1.0, the color of the toluene solution changes from green-brown to green. The band at the longer wavelength is smaller, and both bands in the visible spectrum shift toward the shorter wavelengths (a hypsochromic shift) (Table 2, entry 5). However, at a molar excess of the extractant, $[Cu(II)]_{aq}/[dbim]_{org}$ = 0.5 or 0.1, with a total chloride concentration of 1.0 or 4.0 mol dm^{-3}, the color of the toluene phase after extraction is light green. A bathochromic shift is observed (Table 2, entries 6 and 7). However, at a high molar excess of the extractant, $[Cu(II)]_{aq}/[dbim]_{org}$ = 0.1, and $[Cl^-]_{aq} \leqslant$ 1.0 mol dm^{-3}, the post-extraction toluene phase appears blue. Only one absorption band is observed in the visible range at shorter wavelengths (Table 2, entries 8 and 9).

Table 2 Electronic spectral data for dbim complexes with $CuCl_2$ in toluene solutions ($[dbim]_{org}$ = 0.1 mol dm^{-3} Exp. 1-5 and 7-9; 0.02 mol dm^{-3} -Exp. 6) (sh -shoulder, br -broad band).

Exp. No.	Extraction conditions			The toluene solution at extraction equilibrium		
	$\frac{[Cu(II)]}{[dbim]}$ (mol mol^{-1})	$[NaCl]_{aq}$ (mol dm^{-3})	$[Cl^-]_{aq\ total}$ (mol dm^{-3})	Color	λ_{max} (nm)	ε_{max} (dm^3 mol^{-1} cm^{-1})
1	4.0	4.0	4.8	green-brown	~798 sh 871 br	- 290
2	4.0	0.1	0.9	green-brown	~795 sh 873 br	 216
3	1.0	4.0	4.2	green-brown	~797 sh 863 br	- 250
4	1.0	1.0	1.2	green-brown	~794 sh 870 br	 221

5	1.0	0.1	0.3	green	769 br ~829 sh	167 -
6	0.5	1.0	1.0	light-green	779 br ~858 sh	173 -
7	0.1	4.0	4.0	light-green	805 br	182
8	0.1	1.0	1.0	blue	735	175
9	0.1	0.1	0.1	dark blue	682	160

3.4 Computational Results

In chloride ion containing extraction systems, the structural analysis of copper(II) complexes of 1-alkylbenzimidazole (as a monodentate ligand) shows distinct structures of both mononuclear or dinuclear complexes, where the copper atoms are linked by two μ_2-bridging chloride ions. Starting from simple architectures, we examined the binding stoichiometry of metal and organic ligands reduced to 1-methylbenzimidazole (mbim). We computationally assessed the formation of 1:1 to 1:5 (Cu(II):mbim, mol mol^{-1}) complexes. DFT calculations simplified the number of possible geometries and revealed eight distinct complexes. The optimized structures are represented in Figure 4.

For copper(II) binuclear complexes, molecular orbital analysis is needed to recognize the ground state (a low-spin or high-spin ground state) favored for a dimer containing two weakly interacting metal centers. In the case of complexes **1** and **3**, both doubly bridged species where the bridging ligands are chloride ions, one can analyze the ground state in terms of pairwise interactions of dimeric molecular orbitals. Here, the energy of the Cu(II) dimers gets attention. The energy difference between the lowest energy singlet and triplet states is of fundamental importance, i.e., "singlet−triplet splitting" is an essential factor. In most cases, except for those where overlap between the orbitals takes place, the singlet ground stated is favored. We evaluated the structures of **1** and **3** in both the singlet and triplet states. We found that the triplet states are, respectively 34.2 and 24.8 kcal mol^{-1} more stable than the singlet states. The actual difference in energy may be substantially smaller due to spin delocalization in toluene solvent molecules, which were neglected in the calculations.

For a pair of complexes related to **1** and **3**, containing Cu_2Cl_4, slightly changed geometries were found to display triplet ground states depending upon the geometry when various numbers of benzimidazole ligands (2 or 4) were used (Table 3; Table S1). The bridging Cu-Cl-Cu angles are similar (ca. 93°), although complex **3** with the triplet ground state has a slightly large bridging angle (99.4°) than those of the other complexes. In addition, the lateral Cl atoms in the compounds are twisted out of the molecular plane of the central Cl-Cu-Cl, resulting in loss of planarity in the lateral chloride ions. We do not ascribe much significance to the computed bond angles where the transition from a triplet to singlet ground state occurs since the value is dependent on the choice of complex stereoisomerism.

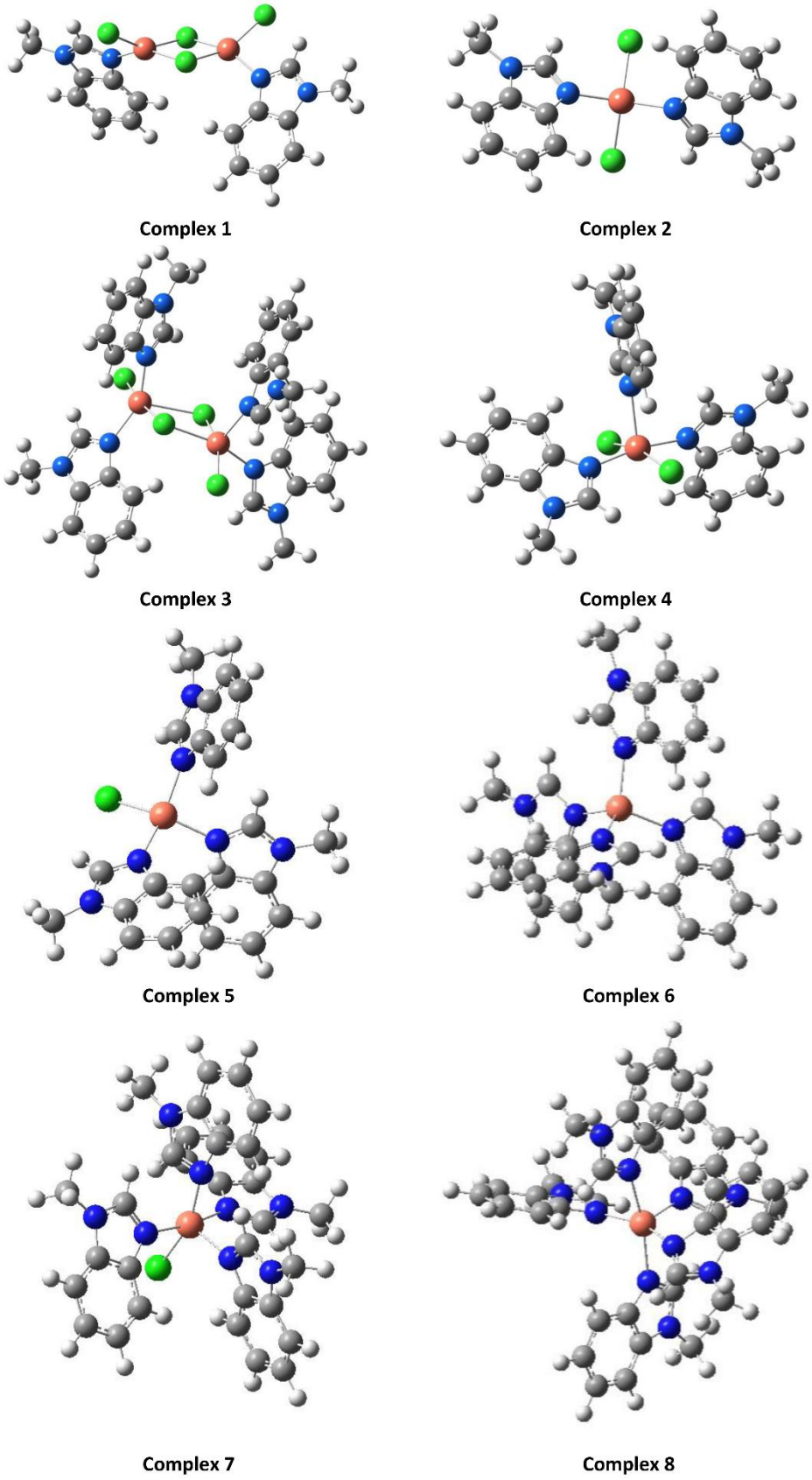

Figure 4 The DFT optimized geometries of mononuclear and binuclear complexes of copper(II) 1-methylbenzimidazole (mbim) molecular structures showing the numbering scheme. All atoms were drawn as spheres of arbitrary radii (orange, copper; gray, carbon; blue, nitrogen; green, chlorine; white, hydrogen).

Table 3 DFT selected bond lengths (in Å), bond angles (in deg.) and torsional angles (in deg.) of 1-methylbenzimidazole complexes **1**-**8**.

Point group[a)]	Bond lengths (Å)		Bond angles (degree)	
	Complex **1**			
C_2 (C_2)	$R_{Cu1-Cu2}$	3.427	∠N1-Cu1-Cl1	95.4
	R_{Cu1-N1}	1.996	∠N1-Cu1-Cl2	154.6
	$R_{Cu1-Cl1}$	2.251	∠N1-Cu1-Cl3	94.4
	$R_{Cu1-Cl2}$	2.334	∠N2-Cu2-Cl2	94.4
	$R_{Cu1-Cl3}$	2.354	∠N2-Cu2-Cl3	154.6
	$R_{Cu2-Cl2}$	2.354	∠N2-Cu2-Cl4	95.4
	$R_{Cu2-Cl3}$	2.334	∠Cu1-Cl2-Cu2	93.9
	$R_{Cu2-Cl4}$	2.251	∠Cu1-Cl3-Cu2	93.9
	R_{Cu2-N2}	1.996	∠N1-Cu1-Cu2-N2	111.3
			BIMA1-BIMA2	62.4
	Complex **2**			
C_2 (C_{2V})	R_{Cu-N1}	2.011	∠N1-Cu-N2	147.4
	R_{Cu-Cl1}	2.296	∠Cl1-Cu-Cl2	143.5
	R_{Cu-Cl2}	2.296	∠BIMA1-BIMA2	82.4
	R_{Cu-N2}	2.011		
	Complex **3**			
C_1 (C_1)	$R_{Cu1-Cu2}$	3.706	∠N1-Cu1-N2	149.3
	R_{Cu1-N1}	2.028	∠N1-Cu1-Cl1	88.8
	R_{Cu1-N2}	2.064	∠N1-Cu1-Cl2	88.6
	$R_{Cu1-Cl1}$	2.348	∠N1-Cu1-Cl3	99.7
	$R_{Cu1-Cl2}$	2.384	∠N3-Cu2-Cl2	94.9
	$R_{Cu1-Cl3}$	2.747	∠N3-Cu2-Cl3	104.3
	$R_{Cu2-Cl2}$	2.473	∠N3-Cu2-Cl4	96.4
	$R_{Cu2-Cl3}$	2.339	∠N3-Cu2-N4	101.9
	$R_{Cu2-Cl4}$	2.350	∠Cu1-Cl2-Cu2	99.4
	R_{Cu2-N3}	2.278	∠Cu1-Cl3-Cu2	93.1
	R_{Cu2-N4}	2.051	∠N1-Cu1-Cu2-N3	0.7
			∠N1-Cu1-Cu2-N4	126.4
			∠N2-Cu1-Cu2-N3	158.4
			∠N2-Cu1-Cu2-N4	74.3
			∠BIMA1-BIMA2	88.6
			∠BIMA3-BIMA4	78.3
	Complex **4**			
C_1 (C_S)	R_{Cu-N1}	2.041	∠N1-Cu-N2	169.4
	R_{Cu-N2}	2.031	∠N1-Cu-N3	98.3
	R_{Cu-N3}	2.359	∠N2-Cu-N3	92.0

	R_{Cu-Cl1}	2.374	∠Cl1-Cu-Cl2	162.3
	R_{Cu-Cl2}	2.402	∠Cl1-Cu-N1	90.7
			∠Cl1-Cu-N2	89.8
			∠Cl1-Cu-N3	95.6
			∠Cl2-Cu-N1	89.4
			∠Cl2-Cu-N2	86.7
			∠Cl2-Cu-N3	101.7
			∠BIMA1-BIMA2	73.6
			∠BIMA2-BIMA3	86.6
			∠BIMA3-BIMA4	84.6
	Complex **5**			
	R_{Cu-Cl}	2.274	∠Cl-Cu-N1	146.6
	R_{Cu-N1}	2.010	∠Cl-Cu-N2	137.4
	R_{Cu-N2}	2.030	∠Cl-Cu-N3	96.7
	R_{Cu-N3}	2.009	∠N1-Cu-N2	96.3
C_1 (C_2)			∠N2-Cu-N3	97.7
			∠N1-Cu-N3	144.9
			∠BIMA1-BIMA2	77.2
			∠BIMA2-BIMA3	73.9
			∠BIMA1-BIMA3	47.2
	Complex **6**			
	R_{Cu-N1}	2.015	∠N1-Cu-N2	94.3
	R_{Cu-N2}	2.006	∠N2-Cu-N3	91.6
	R_{Cu-N3}	2.021	∠N3-Cu-N4	93.0
	R_{Cu-N4}	2.004	∠N4-Cu-N1	92.8
C_1 (S_4)			∠BIMA1-BIMA2	71.0
			∠BIMA1-BIMA3	34.1
			∠BIMA1-BIMA4	76.9
			∠BIMA2-BIMA3	87.3
			∠BIMA2-BIMA4	63.8
			∠BIMA3-BIMA4	89.7
	Complex **7**			
	R_{Cu-Cl}	2.360	∠Cl-Cu-N1	116.8
	R_{Cu-N1}	2.269	∠N1-Cu-N2	87.0
	R_{Cu-N2}	2.047	∠N2-Cu-N3	92.2
	R_{Cu-N3}	2.138	∠N3-Cu-N4	89.5
C_1 (C_2)	R_{Cu-N4}	2.032	∠N4-Cu-Cl	88.3
			∠BIMA1-BIMA2	70.9
			∠BIMA1-BIMA3	47.6
			∠BIMA1-BIMA4	85.2
			∠BIMA2-BIMA3	72.5

			∠BIMA2-BIMA4	83.5
			∠BIMA3-BIMA4	69.8
	Complex **8**			
C_1 (C_4)	R_{Cu-N1}	2.067	∠N1-Cu-N2	92.0
	R_{Cu-N2}	2.042	∠N2-Cu-N3	103.3
	R_{Cu-N3}	2.425	∠N3-Cu-N4	94.3
	R_{Cu-N4}	2.089	∠N4-Cu-N5	88.8
	R_{Cu-N5}	2.064	∠N5-Cu-N1	86.5
			∠BIMA1-BIMA2	70.7
			∠BIMA1-BIMA3	46.6
			∠BIMA1-BIMA4	86.2
			∠BIMA1-BIMA5	68.8
			∠BIMA2-BIMA3	74.9
			∠BIMA2-BIMA4	59.2
			∠BIMA2-BIMA5	50.9
			∠BIMA3-BIMA4	56.4
			∠BIMA3-BIMA5	82.3
			∠BIMA4-BIMA5	88.4

[a)] In parentheses, approximate higher point group determined for metal and ligand electron donor atoms.

In the 1:1 (Cu:mbim) dinuclear complex **1** ($Cu_2Cl_2(mbim)_2(\mu_2\text{-}Cl)_2$) the copper coordination number of 4 is satisfied by a non-alkylated nitrogen atom of 1-methyl benzimidazole (mbim), a chloride ion, and two μ_2-chloride ions forming an approximately square planar rather than the tetrahedral environment around each copper(II) ion. The Cu···Cu nonbonding distance in the complex is 3.427 Å; the two nonbridging bonds Cu1-Cl1 and Cu2-Cl4 are 2.251 Å long, the two shorter bridging Cu1-Cl2 and Cu2-Cl3 bonds are 2.334 Å long, while the two longer Cu1-Cl3 and Cu2-Cl2 bonds are 2.354 Å long. The bridging angle of Cu1-Cl2-Cu2 and Cu1-Cl3-Cu2 is 93.9° (Table 3). Interaction of the C2-H bond of the benzimidazole ligand with the coordinated chloride ions has features of weak hydrogen bonds (length of 2.73 Å, angle of 109°). The double interaction possibly has a stabilizing effect.

The 1:2 (Cu:mbim) stoichiometry can be satisfied by dinuclear coordination, as in the previously discussed complex **3**, ($Cu_2Cl_2(mbim)_4(\mu_2\text{-}Cl)_2$). Both copper(II) centers are five-coordinated, and the structure consists of two combined distorted trigonal bipyramids that share an edge with two bridged chloride ions. Generally, in this arrangement, mbim ligands and chloride ions are sterically hindered. The nonequivalent Cu-N bonds (Cu1-N1 = 2.028 Å, Cu1-N2 = 2.064 Å Cu2-N3 = 2.278 Å Cu2-N4 = 2.051 Å; Table 3) are distinctly longer than the Cu-N bonds in the crystalline dinuclear dichloro-bridged Cu(II) complexes having benzimidazole, 1-methylbenzimidazole, and benzotriazole (1.972-2.020 Å [7, 9, 35]).

Unlike complex **3**, the four-coordinated 1:2 (Cu:mbim), mononuclear complex **2**, and ($CuCl_2(mbim)_2$), are represented as distorted, flattened tetrahedron, having a square planar geometry, with the benzimidazole and chloride ion ligand pairs are *trans* to each other. It is interesting to note that for a 1:2 stoichiometry, the organic ligands complexing the same copper(II)

ion, form two six-membered rings with coordinated chloride ions (Cu ··· N-C-C-H ··· Cl). There is no appreciable strain present in the complexes. Moreover, the angle between the two benzimidazole planes is 82.4°, close to that observed in the π- stacked structure of the benzene dimer (90°). The fused rings are 6.65 Å long and are probably too large to form to π-stacking complexes.

For the 1:3 (Cu:mbim) five-coordinated Cu(II) complex **4** ($CuCl_2(mbim)_3$), the organic ligands are not meridional, contrary to the expectation. The optimized $CuCl_2L_3$ isomer adopts a slightly distorted, square pyramidal shape. The complex has two equatorial, *trans*-oriented chloride ions (Cl1-Cu-Cl2 angle of 162.3°). Two of the three benzimidazole molecules are in opposite corners of the square (N1-Cu-N2 angle of 169.4°). The third organic ligand is present in the axial position of the pyramid (Cu-N3 distance of 2.359 Å). The angles Cl-Cu-N range from 86.7° to 101.7° (Table 3). The twisted orientation of the three benzimidazole moieties is reflected in the angles of 73.6° (for equatorial imidazole planes); 86.6° and 84.8° for axial-equatorial planes.

Complex **5**, ($CuCl(mbim)_3$), has the same metal-benzimidazole stoichiometry as complex **4**, but here, one chloride ion is bound to a four-coordinated copper(II) center. The optimized geometry of complex **5** is an irregular tetrahedral pyramid with metal ions at the vertex and chloride ions placed on the axis perpendicular to the plane of ligand nitrogen atoms. The complex structure **5** has a C1 point group such as **4**. The angles Cl-Cu-N range from 98.2 to 99.8°. The mutual ligand orientation is governed by the orientation of π-electron systems, and it is evident that the planes cut each other at nearly right angles. As in compound **6**, the Cu-N distances of **5** are shorter than those of Cu-Cl by ca 0.4 Å.

Although copper(II) complexes with chloride, benzimidazole or other nitrogen heterocycle ligands in crystalline form are well known [7, 9, 35-40], we predict that during the extraction process, at low chloride ion concentrations, four- or five-coordinated chlorine-free (**6** or **8**, respectively) complexes can be formed. Indeed, in complex **6**, nitrogen atoms of the four benzimidazole ligands are spaced out at the corners of the distorted square, resembling the cyclobutane ring. This is known as the butterfly conformation. The angles of the subsequent nitrogen atoms of the four ligands (N-N-N angles) are 84.5°, 84.8°, 84.5°, and 83.9° (average of 84.4°), while the N-Cu-N angles of the opposite ligands are 153° and 155°. The three-dimensional structure of the five-coordinated metal in **8** strongly resembles that of **6**. Four benzimidazole ligands are arranged in a distorted square (the average N-N-N angle is 90.0°), which forms the base of the tetrahedron with the copper ion at the vertex. The average Cu-N distance of the base ligands is 2.065 Å, which differs significantly from the distance of the fifth distant ligand (2.425 Å).

The architecture of **8** shows two modes of coordination of benzimidazole ligands with the central Cu(II). Therefore we see two kinds of ligands, with the loose ligands being pushed out from the four-coordinated sphere. This leads us to speculate the equilibrium of two geometries and the two coordination modes of chlorine-free complexes at a low concentration or in the absence of chloride ions.

The symmetry of complex **7** is not the same as **6** or **8** (point groups C_2 vs. S_4 and C_4 for **6** and **8**, respectively). The rhombus (with an average N-N-N angle of 81.2°) formed by the four ligand nitrogen atoms is, however, more folded in **7** than in **6**. The copper(II) ion lies in the middle of the alternating nitrogen ligands (the N-Cu-N angle is 177°, R_{Cu-N} = 2.04 Å). The complementary pair of ligands exhibit a weaker bond (115° and 2.2 Å). The fifth ligand, a chloride ion, is located on the axis of the tetrahedron, 2.36 Å away from the copper ion. Undoubtedly, chloride ions in **7** fill up the free space of five-coordination driven by the geometric preference of metal ions.

4. Discussion

4.1 Results of Extraction Studies

Although dbim has a strong affinity for hydrogen ions in an acidic media (Table 1, Chapter 3.1), it can be assumed that the extraction of Cu(II) by dbim (0.1 mol dm^{-3}) from weakly acidic chloride solutions (pH > 2.2) can be described according to Eq. (4):

$$mCu^{2+}{}_{aq} + 2mCl^{-}{}_{aq} + nL_{org} = (CuCl_2)_m L_{n,org} \quad (4)$$

L -the solvating extractant dbim.

The copper(II) extraction studies show (Figure 3, Chapter 3.2) that at the molar ratio of $[Cu(II)]_{aq}/[dbim]_{org} \geq 1.0$ and $[Cl^-]_{aq} \geq 0.9$ mol dm^{-3}, in toluene, $(CuCl_2)_m(dbim)_n$ complexes with an m:n ratio equal to 1:2 or 1:1, can form because the capacity of dbim is greater than 0.5 mol Cu/mol extractant.

After Cu(II) extraction, the two absorption bands observed in the visible region for the spectra of toluene, when $[Cu(II)]_{aq}/[dbim]_{org}$ = 0.5-4.0 mol mol^{-1} (Table 2, Chapter 3.3), suggest that in the complexes formed during these extraction processes, the central ion, Cu(II), is coordinated to at least three chloride ions [41, 42]. This indicates that chloride bridges exist between copper ions. The band maxima are in agreement with the two maxima observed in the visible spectrum of the $CuCl_2$ complex with *N*,*N*-diethylpyridine-3-carboxamide in methylene chloride or nitrobenzene (775 and 850 nm) [41]. Davies et al. proved that this complex is a dimer with two chloride bridges and a trigonal bipyramidal coordination environment around two metal ions. The molar ratio of copper(II) to the organic ligand is 1:2. However, Rodriguez-Fortea and coworkers [43] reported that in dihalo-bridged Cu(II) complexes, the metal ions are usually four- or five-coordinated, and a square-planar (in some cases a tetrahedral) or a square-pyramidal (rarely a trigonal bipyramidal) geometry is observed, respectively. This indicates that dbim-$CuCl_2$ complexes with different geometry may be formed in the extraction systems where the molar ratio of Cu(II):dbim may vary from 1:1 to 1:2.

However, when the extractant is in large excess with respect to copper(II) (10:1) and $[Cl^-]_{aq} \leq 1.0$ mol dm^{-3}, one absorption band is observed in the visible region (Table 2, entries 8 and 9). It can be assumed that the complexes that are formed under these conditions have no chloride bridges. Davies et al. [41] observed the same changes in the spectra of amide complexes synthesized in the presence of excess ligands and proposed that these $CuCl_2L_3$ (L -organic ligand) complexes are monomeric.

The experimental results indicate that the structure of complexes formed in the extraction process strongly depends on the extraction conditions. It seems that when $[Cu(II)]_{aq}/[dbim]_{org}$ = 1-4 mol mol^{-1}, in the extraction processes, even a small excess of the extractant, can form complexes with chloride bridges where the molar ratio of Cu(II):dbim varies from 1:1 to 1:2 (Table 2, entries 1-6). However, at a significant molar excess of the extractant, depending on the extraction system chloride concentration, 1:2 and 1:3 complexes (Cu(II):dbim, mol mol^{-1}) are in equilibrium through the chloride ion-dbim exchange (Table 2, entries 7-9).

4.2 Comparison of the Stability of the Computational Structures Proposed for $CuCl_2$-mbim Complexes

The DFT-PCM total energies (in Hartree), calculated at B3LYP/6-31++G(d,p) of the four optimized complexes, are detailed in Table S2 (Supporting Information). The different stoichiometries of these complexes make their simple comparison difficult. The exceptions are the mononuclear complex **2** and the binuclear complex **3**, where the structure of the latter is the dimer of the former. In toluene, complex **3** is 5.10 kcal mol^{-1} less stable than two molecules of complex **2** (5.66 kcal mol^{-1} in water and 6.39 kcal mol^{-1} in a vacuum). However, this comparison is meaningless based on the X-ray structure analysis because of the complete absence of the structural motifs of complex **2** and the likely impact of the scheme of complex **3**.

To account for a compact structure, nonbridging Cu-Cl and bridging Cu-Cl bond lengths were chosen as key attributes, based on which the comparison of the structures was made. A structural comparison of complexes **3** and **4,** both five-coordinated copper species, and complex **1**, a four-coordinated copper(II) complex, demonstrates that all the Cu-N, nonbridging Cu-Cl and bridging Cu-Cl bond lengths in the five-coordinated copper(II) models are distinctly longer (and probably weaker) than those in complex **1**. These appeared to be the most compact dimensions in terms of the lengths of the individual bonds. The average Cu-N bond lengths are 1.996, 2.046/2.165, and 2.144 Å for complexes **1, 3**, and **4,** respectively. In the same order, the nonbridging Cu-Cl distances are 2.251, 2.349, and 2.388 Å. Similarly, the bridging Cu-Cl bond lengths are 2.334 and 2.488 Å (Table 3). There were subtle differences in the parameters used. Hence, the geometric criterion, mentioned above, for selecting the most stable structures for complexes **2** and **1** should not be used. This is the case when there are some difficulties in harmonizing the subtle relationship between the alternative coordination modes of copper(II) as a four- or five-coordinated center in mono- and binuclear complexes.

The mononuclear complexes with coordination numbers 4, 5, and 6 typically have a tetrahedral geometry. For benzimidazole ligands, Cu-N bond lengths are ca. 2.02 Å (in **2**), while for Cu-Cl of **5,** even 2.00 Å. It seems that a coordination number of four is the natural coordination number of the discussed complexes, while the higher coordination number appears to reflect the higher affinity of Cu(II) to chloride anion compared to the bulkier benzimidazole ligands. The coordination number of five is probably preferred with high ligand excess (benzimidazole/ chloride, or both) toward metal ion, and then complexes **4**, **7**, or **8** are formed. The analysis of the structural data (Table 3) leads to the conclusion that excessive ligand and crowding in the first coordination sphere leads to a displacement of the benzimidazole moiety. The extent of displacement is about 0.2 Å in **7**, 0.3 Å in **4**, and 0.4 Å even in the most crowded complex **8**. It is evident that the affinity of benzimidazole, as an electron donor and its steric requirements, makes neutral organic ligands less attractive as coordinating centers than the chloride ion.

4.3 Comparison of Experimental and TD-DFT Calculated Visible Spectra of $CuCl_2$ Complexes with 1-Alkylbenzimidazoles and Other Heteroaromatic Ligands

As shown in Chapter 4.1 and Table 2, in the extraction process, the visible spectra for $CuCl_2$ complexes with dbim in toluene do not represent the formation of a single complex. They rather indicate the formation of multiple complexes with a change in extraction conditions.

In the presence of chloride ions, at $[Cu(II)]_{aq}/[dbim]_{org} \geq 1.0$ mol mol^{-1}, and even with a small excess of the extractant, complexes formed in the extraction systems probably have chloride bridges between copper ions. However, the stereochemistry of copper(II) in these complexes depends on both upon the chloride ion concentration in the aqueous phase and the molar ratio of $[Cu(II)]_{aq}/[extractant]_{org}$ in the extraction system.

It should be noted that at $[Cu(II)]_{aq}/[dbim]_{org} \geq 1.0$ mol mol^{-1} and $[Cl^-]_{aq} \geq 0.9$ mol dm^{-3} (Table 2, entries 1-4), in the visible spectra of the toluene phase, two bands at low intensities are observed for *d-d* transitions: a broad band at 863-873 nm and a lower-intensity shoulder in the 794-798 nm region. Similar bands for the *d-d* transitions appear in the spectra of $CuCl_2$ complexes with pyridine and its derivatives: 4-methyl- and 3-methylpyridine (diluent - CH_2Cl_2) 830-847 nm (the broad band) and 760-784 nm (the shoulder) [44]. Based on X-ray studies [45, 46], it was shown that in these complexes, the octahedral polymeric structure is formed by "the based planes of copper(II)" connected with chloride bridges. As shown in Table 4, the lengths of the Cu-N and the $Cu\text{-}Cl_{equatorial}$ bonds in these complexes are comparable to the lengths calculated for the corresponding bonds in complex **1** (Figure 4), with square planar geometry and chloride bridges. In the region corresponding to λ > 700 nm in TD-DFT- calculated visible spectra of complex **1** (Table S4 -Supplementary Information), there are four bands with varying intensities in the order of 885 > 744 > 729 > 934 nm. However, in the region corresponding to λ > 700 nm in the TD-DFT-calculated spectra of complexes **2** and **3** (Table S4), the observed bands have lower intensity than that of complex **1**. However, in the 500-600 nm range, there are bands of significant intensity, which are not observed in either the experimental (Table 2) or the calculated spectra for complex **1**. Similarities between calculated and experimental data in the visible electronic spectra at λ > 700 nm may indicate that only a square planar dual-core complex **1**, is responsible for the observed properties of the extraction at $[Cu(II)]_{aq}/[dbim]_{org} \geq 1.0$ mol mol^{-1} and $[Cl^-]_{aq} \geq 0.9$ mol dm^{-3}.

Table 4 Cu-N and Cu-Cl bond lengths in square-planar complexes (eq -equatorial, ax - axial).

No.	Complex	Bond lengths (Å)				Lit.
		$Cu\text{-}N_{eq}$	terminal $Cu\text{-}Cl_{eq}$	bridging $Cu\text{-}Cl_{eq}$	bridging $Cu\text{-}Cl_{ax}$	
1	**Complex 1 $Cu_2Cl_4(mbim)_2$**	1.996	2.251	2.334/2.354	-	this work
2	**Square-planar $CuCl_2L_2$**					
2a	L = 4-ethylpyridine	2.00	2.28	-	-	[36]
2b	L = 2,3-dimethylpyridine	1.977	2.254	-	-	[39]
2c	L = 2-(2,4-difluorophenyl)pyridine	1.9997	2.2713	-	-	[40]
3	**$(CuCl_2L_2)_n$ octahedral polymeric structure with chloride bridges**					
3a	L = pyridine	2.02	-	2.28	3.05	[45]
3b	L = 4-methylpyridine	2.07	-	2.35	3.19	[46]

However, at $[Cu(II)]_{aq}/[dbim]_{org}$ = 1.0 mol mol^{-1} and a low chloride concentration (0.3 mol dm^{-3}), (or with a small excess of the extractant ($[Cu(II)]_{aq}/[dbim]_{org}$ = 0.5 mol mol^{-1})) (Table 2, entries 5 and 6), the visible spectra of toluene solutions after the Cu(II) extraction consists of a relatively intense band at ca. 770-780 nm and a lower intensity shoulder ca 830-860 nm. It can be assumed that under the applied extraction conditions, the stereochemistry around the metal ion changes. Davies and coworkers [41] obtained very similar band maxima (775 and 850 nm) in the spectra of the $CuCl_2$ complex with *N, N*-dietylpyridine-3-carboxamide in organic solvents. They showed that in the dimer having two chloride bridges, copper(II) is five-coordinated. A trigonal bipyramidal environment around the two metal ions is observed, and the molar ratio of copper(II) to the organic ligand is 1:2. However, TD-DFT-calculated spectra of the complex **3** (Table S4), carried out for multiplicity 1 and multiplicity 3, showed significant differences. Unlike multiplicity 1, multiplicity 3 showed two notable bands at λ > 700 nm (765 and 836 nm). For multiplicity 1, the bands in the 500-600 nm region have much lower intensity. The TD-DFT-calculated spectra of complex **3** (multiplicity 3) (Table S4) suggest that at these experimental conditions (Table 2, entries 5 and 6), complexes with 1:2 stoichiometry may be formed. The authors compared the dinuclear dichloro-bridging geometry of complex **3** with the geometry of the $[cis\text{-}CuCl_2(DMF)_2]_2$ dimer [47]. X-ray analysis of the DMF complex showed that each bridging Cl atom is coordinated to two Cu(II) ions. In one coordination sphere, it occupies an axial position, and in the other, it occupies an equatorial position. In the equatorial plane of the trigonal bipyramids in complex **3**, three equatorial bonds of different lengths and three different angles N(or Cl)-Cu-N(or Cl) are observed (Table 3). X-ray diffraction studies for the DMF complex also showed such differences.

As shown in Chapter 4.1, at a large molar excess of the extractant to copper(II), (Table 2, items 7-9), only one band is observed at λ > 450 nm in the electronic spectra of the toluene solution despite the presence of chloride ions. This indicates that in the copper(II) complexes, there are no chloride bridges. Besides, the band in the 680-805 nm region suggests that these are monomeric complexes of the form $CuCl_2(dbim)_3$, similar to that of complexes formed in when $CuCl_2$ reacts with an excess of *N, N*-diethylpyridine-3-carboxamide [41]. A single band at 760 nm (CH_2Cl_2) was also observed for these pyridine derivatives. The EPR spectra showed that the structure of the complexes took a trigonal bipyramidal or square pyramidal geometry, depending on the temperature. However, although TD-DFT-calculated spectrum of complex **4**, with a five-coordinated copper(II) center, showed a band at λ > 700 nm, in reality, one band at 772.72 nm was observed (Table S4). It should be noted that in the 450-520 nm region of the calculated spectrum, three additional bands are generated that are unfortunately not apparent in the spectrum of the toluene phase obtained after extraction. The experimental and the calculated spectra are not in good agreement. However, given the high similarity between the predicted DFT-calculated molecular structure of complex **4** and the tetragonal pyramid structure of the $CuCl_2$ complexes with 4-methylthiazole and 2-methylpyridine (Table 5, X-ray data), and the experimental spectra of dbim and *N, N*-diethylpyridine-3-carboxamide complexes, it can be assumed that at excess 1-alkylbenzimidazole with respect to copper(II) ions, monomeric complexes with 1:3 (Cu:dbim) stoichiometry can be formed in systems containing chloride ions even when chloride ions are in excess (Table 2, entries 7-9). However, the formation of complexes with a molar ratio of organic ligand: copper(II) molar ratio > 3 cannot be excluded.

Table 5 Comparison of complex **4** structure with X-ray data for the $CuCl_2L_3$ and $CuCl_2L_2(OH_2)$ (L -an organic ligand) complexes with a tetragonal pyramid structure (eq - equatorial, ax -axial).

Bond lengths (Å) and internuclear angles (deg)	Complex **4** $CuCl_2(mbim)_3$	$CuCl_2$(4-methylthiazole)$_3$	$CuCl_2$(2-methylpyridine)$_2(OH_2)$
	[this work]	[38]	[37]
trans Cl(1)-Cu-Cl(2)	162.3	-	173.66
trans N(1)-Cu-N(2)	169.4	169.53	173.98
trans Cl(2)-Cu-N(3)	-	153.03	-
Cu-Cl(1)eq	2.374	-	2.314
Cu-Cl(2)eq	2.402	2.319	2.296
Cu-Cl(1)ax	-	2.461	-
Cu-N(1)eq	2.041	2.043	2.013
Cu-N(2)eq	2.031	2.066	2.016
Cu-N(3)ax	2.359	-	-

Based on the analysis of the experimental, computational, and literature data, it is necessary to group the results of experiments 1-9 (Table 2), taking into account a simplified classification of the [Cu(II)]/[dbim] molar ratio and the total concentration of chloride ions ($[Cl^-]_{aq}$) (Table 6). Within the series of extraction experiments, we assume that the ratio [Cu(II)]/[dbim] varies from high (4.0-1.0 mol mol^{-1}), medium (1.0-0.1 mol mol^{-1}) to low (ca 0.1 mol mol^{-1}). Similarly, the total chloride ion concentration differs nearly 50 times from high (ca 4.8-1.0 mol dm^{-3}) to low (ca 0.1 mol dm^{-3}). The law of mass action suggests that the high concentration of chloride favors the formation of binuclear, bridged species such as **1** or **3**. Complex **2** is formed to some extent, while complex **4** is hardly formed. In contrast, at the low concentration of chloride ions and a very low ratio of [Cu(II)]/[dbim] (which means a significant excess of organic ligand to copper ions), complexes **6** and/or **8** are probably formed. It is not clear whether complex **7** participates in equilibrium. The absorption data of visible spectrum for [Cu(II)]/[dbim] = 0.1 mol mol^{-1} and $[Cl^-]_{aq}$ = 1.0 mol dm^{-3} are consistent with the computer-calculated TD excitation energy of complex **4**.

Table 6 TD interpretation of visible spectra of dbim complexes with $CuCl_2$ in toluene solutions.

Extraction conditions		Experimental UV/VIS spectra		Calculated UV/VIS spectra		
$\frac{[Cu(II)]}{[dbim]}$ (mol mol^{-1})	$[Cl^-]_{aq\ total}$ (mol dm^{-3})	λ_{max} (nm)	ε_{max} (dm^3 mol^{-1} cm^{-1})	TD λ_{max}^{calc} (nm)	f	Suggested structure
4.0-1.0	4.8-0.9	798-794 sh 873-863 br	220-290	729 744 885	0.0028 0.0030 0.0052	**1**
0.1-1.0	0.3-4.0	769-805 br 829-858 sh	160-180	765 836	0.0035 0.0046	**3**[a] and/or **5**

				753	0.0026	
				815	0.0036	
0.1	1.0	735	175	773	0.0025	**4**
				738	0.0007	
				681	0.0020	**6**
				632	0.0012	
				611	0.0073	
0.1	0.1	682	160			and/or
				682	0.0020	
				651	0.0017	**8**
				614	0.0016	

[a)] **3**(multiplicity 3) with contribution of **3a**(multiplicity 1) or additionally **7** (for TD λ_{max}^{calc} and f data see Table S4)

5. Conclusions

In summary, we have demonstrated for the first time that 1-decylbenzimidazole forms several mono- and binuclear complexes with copper(II) with coordination numbers of 4 or 5. We have presented a detailed DFT structural study on the coordination property of Cu(II) ions toward 1-methylbenzimidazole ligands and confirmed the existence of 1-decylbenzimidazole complexes, in toluene solutions. We have shown that manipulation of both the [Cu(II)]/[dbim] and the chloride ion concentration can reversibly modulate copper(II) nuclearity as well as its coordination number. 1-Decylbenzimidazole (dbim) can form a binuclear square planar 1:1 complex $[Cu_2Cl_4(dbim)_2]$, binuclear 1:2 complex $[Cu_2Cl_4(dbim)_4]$ (distorted trigonal-bipyramidal geometry), and $[CuCl_2(dbim)_3]$, $[Cu(dbim)_4]Cl_2$ or $[Cu(dbim)_5]Cl_2$ complexes, with four- or five-coordinated copper(II) centers, depending on the extraction conditions.

Conclusions about the coordination of the ligands in adducts have been made by comparing their simulated structures with the corresponding X-ray multidimensional architectures of ligands reported in the literature. A critical evaluation of the results was discussed in terms of the specific dbim structural factors. Bond lengths in the computed complexes are alternatively used as an essential and sensitive reporter of the ligand field strength and anticipated stability of coordinated imine (as 1-alkylbenzimidazole) and chloride ions. Unfortunately, the recorded visible spectra and the calculated TD-DFT spectra for the models were not in good agreement. Nevertheless, the tested model structures were employed to distinguish chemically important complexes from irrelevant ones.

Additional Materials

The following additional materials are uploaded on the page of this paper.

1. Table S1: The comparison of selected geometrical parameters (bond lengths (in Å), bond angles (in deg.)) of singlet and triplet structures of 1-methylbenzimidazole **1** and **3** complexes at B3LYP/6-31++G(d,p) level of theory calculated in the toluene phase with the IEF-PCM solvation model.

2. Table S2: Coordinates of structures **1**-**8** of Cu(II) complexes with chloride ions and 1-methylbenzimidazole in toluene at the B3LYP/6-31++G(d,p) level of theory.

3. Table S3: Absolute and relative energies for singlet and triplet of binuclear 1-methylbenzimidazole copper(II) complexes for structures of **1** and **3** at B3LYP/6-31++G(d,p) level of theory calculated in the toluene phase with the IEF-PCM solvation model.

4. Table S4: Calculated TD-DFT spectra of structure **1-8** of Cu(II) complexes with chloride ions and 1-methylbenzimidazole in toluene at the B3LYP/6-31++G(d,p) level of theory. Excitation energies and oscillator strengths: 900nm > λ > 600nm, f > 0.002.

Author Contributions

All authors are equally contributed.

Funding

The work was supported by the Polish Ministry of Science and Higher Education.

Competing Interests

The authors have declared that no competing interests exist.

References

1. Şahin E, İde SE, Kurt M, Yurdakul Ş. Structural investigation of dichlorobis (benzimidazole) Zn(II) complex. Z Kristallogr Cryst Mater. 2003; 218: 385-387.
2. Yoe-Reyes FJ, Bernès S, Barba-Behrens N. Dichlorobis(1*H*-benzimidazole-*κN*3) cobalt(II). Acta Crystallogr C. 2005; 61: m875-m877.
3. Bukowska-Strzyżewska M, Tosik A. Crystal and molecular structure of dibromobis (benzimidazole) copper(II): A low-temperature investigation. J Crystallogr Spectrosc Res. 1991; 21: 379-383.
4. Sánchez-Guadarrama O, López-Sandoval H, Sánchez-Bartéz F, Gracia-Mora I, Höpfl H, Barba-Behrens N. Cytotoxic activity, X-ray crystal structures and spectroscopic characterization of cobalt(II), copper(II) and zinc(II) coordination compounds with 2-substituted benzimidazoles. J Inorg Biochem. 2009; 103: 1204-1213.
5. Mohamed GB, Masoud MS, Hindawey AM, Obeid NA. Ligation properties of some imidazole compounds. Rev Inorg Chem. 1992: 81-94.
6. Şjrecį N, Yilmaz Ü, Küçükbay H, Akkurt M, Baktir Z, Türktekin S, et al. Synthesis of 1-substituted benzimidazole metal complexes and structural characterization of dichlorobis(1-phenyl-1*H*-benzimidazole-κN^3) cobalt (II) and dichlorobis (1-phenyl-1*H*-benzimidazole- κN^3) zinc (II). J Coord Chem. 2011; 64: 1894-1902.
7. Tosik A, Maniukiewicz W, Bukowska-Strzyżewska M, Mroziński J, Sigalas MP, Tsipis CA. A new structural type for a binuclear chloride-bridged copper (II) complex. Structural and magnetic characterization of di-μ-chloro-chloropentakis (benzimidazole)dicopper (II) monochloride tetrahydrate, $[Cu_2Cl_3(C_7H_6N_2)_5]Cl{\cdot}4H_2O$. Inorg Chim Acta. 1991; 190: 193-203.
8. Tosik A, Bukowska-Strzyżewska M. Crystal and molecular structure of di-μ-bromobromopentakis(benzimidazole)dicopper(II) monobromide tetrahydrate $[Cu_2Br_3(C_7H_6N_2)_5]Br{\cdot}4H_2O$. J Chem Crystall. 1994; 24: 139-143.

9. Jeong DH, Park WJ, Jeong JH, Churchill DG, Lee H. Facile N-N coupling and copper (II) promoted cleavage of *N*,*N*'-linked *N*-methylbenzimidazole. Inorg Chem Commun. 2008; 11: 1170-1173.
10. Goodgame M, Haines LI. Copper(II) complexes of benzimidazole. J Chem Soc A. 1966: 174-177.
11. Devonald DP, Nelson AJ, Quan PM, Steward D. Process for the extraction of metal values and novel metal extractants. Eur Patent Spec. 1986; 0 193 307 B1.
12. Matthews CJ, Leese TA, Clegg W, Elsegood MR, Horsburgh L, Lockhart JC. A route to bis(benzimidazole) ligands with built-in asymmetry: Potential models of protein binding sites having histidines of different basicity. Inorg Chem. 1996; 35: 7563-7571.
13. Kinnear KI, Lockhart JC, Rushton DJ. Selectivity in transport. J Chem Soc Dalton Trans. 1990; 1365-1373.
14. Lockhart JC, Rushton DJ. Silver selectivity: A study of metal recognition in single and multiple phases. J Chem Soc Dalton Trans. 1991; 2633-2638. Doi: 10.1039/DT9910002633.
15. Matthews CJ, Leese TA, Thorp D, Lockhart JC. Three-phase transport studies of benzimidazole ligands bearing hydrophobic *N*-alkyl substituents: Transport of metal(II) ions (Ni, Cu, Zn, Cd) in single- and multiple-ion experiments. J Chem Soc Dalton Trans. 1998; 79-88. Doi: 10.1039/A705387H.
16. Zhong YR, Cao ML, Mo HJ, Ye BH. Syntheses and crystal structures of metal complexes with 2,2'-biimidazole-like ligand and chloride: Investigation of X—H···Cl (X = N, O, and C) hydrogen bonding and Cl—π (imidazolyl) interactions. Cryst Growth Des. 2008; 8: 2282-2290.
17. Stibrany RT. Exploration of benzimidazole chemistry. New Jersey: The State University of New Jersey; 2008.
18. Cote G, Jakubiak A, Bauer D, Szymanowski J, Mokili B, Poitrenaud C. Modelling of extraction equilibrium for copper(II) extraction by pyridine-carboxylic acid ester from concentrated chloride solutions at constant water activity and constant total concentration of ionic or molecular species dissolved in the aqueous solution. Solvent Extr Ion Exch. 1994; 12: 99-120.
19. Mack J, Sosa-Vargas L, Coles SJ, Tizzard GJ, Chambrier I, Cammidge AN, et al. Synthesis, characterization, MCD spectroscopy, and TD-DFT calculations of copper-metalated nonperipherally substituted octaoctyl derivatives of tetrabenzotriazaporphyrin, cis- and transtetrabenzodiazaporphyrin, tetrabenzomonoazaporphyrin, and tetrabenzoporphyrin. Inorg Chem. 2012; 51: 12820-12833.
20. Jesser A, Rohrmüller M, Schmidt WG, Herres-Pawlis S. Geometrical and optical benchmarking of copperguanidine-quinoline complexes: Insights from TD-DFT and many-body perturbation theory. J Comput Chem. 2014; 35: 1-17.
21. Scalmani G, Frisch MJ. Continuous surface charge polarizable continuum models of solvation. I. General formalism. J Chem Phys. 2010; 132: 114110.
22. Adamo C, Jacquemin D. The calculations of excited-state properties with time-dependent density functional theory. Chem Soc Rev. 2013; 42: 845-856.
23. Stratmann RE, Scuseria GE, Frisch MJ. An efficient implementation of time-dependent density-functional theory for the calculation of excitation energies of large molecules. J Chem Phys. 1998; 109: 8218-8224.
24. Jacquemin D, Adamo C. Computational molecular electronic spectroscopy with TD-DFT. Top Curr Chem. 2016; 368: 347-375.
25. Pellegrin Y, Sandroni M, Blart E, Planchat A, Evain M, Bera NC, et al. New heteroleptic bis-phenanthroline copper(I) complexes with dipyridophenazine or imidazole fused

phenanthroline ligands: Spectral, electrochemical, and quantum chemical studies. Inorg Chem. 2011; 50: 11309-11322.
26. Fumanal M, Daniel C. Description of excited states in [Re(Imidazole)(CO)3(Phen)]$^{+}$ including solvent and spin-orbit coupling effects: density functional theory versus multiconfigurational wavefunction approach. J Comput Chem. 2016; 37: 2454-2466.
27. Borowiak-Resterna A, Chlebowska H, Giezek M. Zinc extraction from chloride solutions with *N*-alkyl- and *N*,*N*-dialkylpyridinecarboxamides. Hydrometallurgy**.** 2010; 103: 158-166.
28. Mądrzak-Litwa I, Borowiak-Resterna A. Solvent extraction of zinc from chloride solutions using dialkyl derivatives of 2,2'-bibenzimidazole as extractants. Hydrometallurgy**.** 2018; 182: 8-20.
29. Mądrzak-Litwa I, Borowiak-Resterna A. Solvent extraction of copper(II) from chloride solutions using 1,1'-dialkyl-2,2'-bibenzimidazoles as extractants. Physicochem Probl Mineral Pro. 2019; 55: 1165-1178.
30. Nave S, Mandin C, Martinet L, Berthon L, Testard F, Madic C, et al. Supramolecular organisation of tri-n-butyl phosphate in organic diluent on approaching third phase transition. Phys Chem Chem Phys. 2004; 6: 799-808.
31. Steck EA, Nachod FC, Ewing GW, Gorman NH. Absorption spectra of heterocyclic compounds. III. Some benzimidazole derivatives. J Am Chem Soc. 1948; 70: 3406-3410.
32. Du Preez JG. Recent advances in amines as separating agents for metal ions. Solvent Extr Ion Exch. 2000; 18: 679-701.
33. Bullock JI, Choi SS, Goodrick DA, Tuck DG, Woodhouse EJ. Organic phase species in the extraction of mineral acids by methyldioctylamine in chloroform. J Phys Chem. 1964; 68: 2687-2696.
34. Davis AR, Chong C. Laser Raman study of aqueous copper nitrate solutions. Inorg Chem. 1972; 11: 1891-1895.
35. Søtofte I, Nielsen K. Benzotriazole complexes. I. The crystal structure of di-μ-chloro-bis[bis(benzotriazole)chlorocopper(II)] monohydrate. Acta Chem Scand A. 1981; 35: 733-738.
36. Laing M, Carr G. Crystal and molecular structure of dichlorobis-(4-ethylpyridine)-copper(II). J Chem Soc A Inorg Phys Theor. 1971: 1141-1144.
37. Marsh WE, Hatfield WE, Hodgson DJ. Magnetic interactions in chloro-bridged dimers. Structural characterization of aquadichlorobis(2-methylpyridine)copper(II) and bis[dichlorobis(2-methylpyridine)copper(II)]. Inorg Chem. 1982; 21: 2679-2684.
38. Marsh WE, Hatfield WE, Hodgson DJ. Structural characterization of dimeric and monomeric copper(II) complexes of 4-methylthiazole. Inorg Chem. 1988; 27: 1819-1822.
39. Stählin W, Oswald HR. The crystal structures of dichlorobis-(2,3-dimethylpyridine)copper(II) and dibromobis-(2,3-dimethylpyridine)copper(II). Acta Crystallogr B. 1971; 27: 1368-1373.
40. Vural H, İdil Ö. Synthesis, spectroscopic investigation and biological activities of copper(II) complex of 2-(2,4-difluorophenyl)pyridine: A combined theoretical and experimental study. J Mol Struct. 2019; 1177: 242-248.
41. Davies G, El-Toukhy A, Onan KD, Veidis M. Synthesis, structure and properties of the isomeric dinuclear complexes $[(DENC)_2CuX_2]_2$ (DENC = *N*,*N*-diethylnicotinamide; X = Cl or Br) and the kinetics of their reactions with DENC in methylene chloride. Inorg Chim Acta. 1985; 98: 85-94.
42. Tom Dieck H. Tetranuclear complexes of trigonal-bipyramidal copper(II). III. Electronic and infrared spectra. Inorg Chim Acta. 1973; 7: 397-403.

43. Rodriguez-Fortea A, Alemany P, Alvarez S, Ruiz E. Exchange coupling in hal-bridged dinuclear Cu(II) compounds: A density functional study. Inorg Chem. 2002; 41: 3769-3778.
44. Ludwig W, Gasser F. Darstellung und spektroskopische untersuchungen von kupferkomplexen mit verschiedenen mikrostrukturen. I. halogeno- stickstoffbasen-kupfer(II)-komplexe. Helv Chim Acta. 1969; 52: 107-121.
45. Dunitz JD. The crystal structures of copper dipyridine dichloride and the violet form of cobalt dipyridine dichloride. Acta Crystallogr. 1957; 10: 307-313.
46. Marsh WE, Valente EJ, Hodgson DJ. Structure of bis-(4-methylpyridine)dichlorocopper(II): A dislocated linear chain. Inorg Chim Acta. 1981; 51: 49-53.
47. Lavrentiev IP, Korableva LG, Lavrentieva EA, Nifontova GA, Khidekel ML, Gusakovskaya IG, et al. Liquid phase oxidation of transition metals. Part 6. Iron and copper complexes containing dimethylsulphoxide, dimethylformamide, and acetonitrile. Anomalous states of ligands. Transition Met Chem. 1980; 5: 193-200.